TUTDoR

Computational investigation of the interaction mechanisms of low-density polyethylene (LDPE)/polyurethane and low-density polyethylene (LDPE)/hexane systems as absorbents for oil spill remediation: A DFT study.

Item Type	Article
Authors	Odera, Raphael Stone.;Ezika, Anthony Chidi.;Adekoya, Gbolahan Joseph.;Sadiku, Emmanuel Rotimi.;Okpechi, Victor Ugochukwu.;Oyeoka, Henry Chukwuka.
Publisher	Wiley
Rights	Attribution-NoDerivatives 4.0 International
Download date	2025-07-03 20:43:31
Item License	http://creativecommons.org/licenses/by-nd/4.0/
Link to Item	https://hdl.handle.net/20.500.14519/365

RESEARCH ARTICLE

Computational investigation of the interaction mechanisms of low-density polyethylene (LDPE)/polyurethane and low-density polyethylene (LDPE)/hexane systems as absorbents for oil spill remediation: A DFT study

Raphael Stone Odera[1] | Anthony Chidi Ezika[2] | Gbolahan Joseph Adekoya[2] |
Emmanuel Rotimi Sadiku[2] | Victor Ugochukwu Okpechi[1] |
Henry Chukwuka Oyeoka[1]

[1]Department of Polymer Engineering, Faculty of Engineering, Nnamdi Azikiwe University, Awka, Nigeria

[2]Institute of Nanoengineering Research (INER) & Department of Chemical, Metallurgical and Materials Engineering, Faculty of Engineering and the Built Environment, Tshwane University of Technology, Pretoria, South Africa

Correspondence

Anthony Chidi Ezika, Institute of Nanoengineering Research (INER) & Department of Chemical, Metallurgical and Materials Engineering, Faculty of Engineering and the Built Environment, Tshwane University of Technology, Pretoria 0001, South Africa.
Email: tonero2017@gmail.com

Abstract

The escalating frequency of oil spill incidents and industrial wastewater discharges necessitates the development of effective remediation strategies. In this study, we conduct a comprehensive computational investigation using density functional theory (DFT) to elucidate the interaction mechanisms within polyethylene (PE) combined with polyurethane (PU) and hexane. The study focuses on adsorption energies, intermolecular interactions, miscibility, and electronic properties, providing a molecular-level understanding crucial for designing advanced absorbent materials. The investigation reveals that the low-density polyethylene/polyurethane (LDPE/PU) system exhibits significantly higher adsorption energies (-12.87 kcal/mol) compared to PE/hexane (-7.66 kcal/mol), indicating a robust binding affinity. This discrepancy underscores the superior performance of PE/PU as an absorbent material. The enthalpy results, with ΔH values of -55.75 kcal/mol for PE/hexane-n-hexadecane and -66.11 kcal/mol for PE/PU-n-hexadecane complexes at 298.15 K, support exothermic adsorption. The more exothermic ΔH for PE/PU indicates stronger interactions during oil absorption than PE/hexane. Additionally, Gibbs free energy change (ΔG) values affirm a more favorable process for PE/PU, exhibiting a lower ΔG (-42.54 kcal/mol) compared to PE/hexane (-34.79 kcal/mol). Non-covalent interaction (NCI) studies confirm the importance of van der Waals forces in both systems, validating their role in the adsorption process. Miscibility studies indicate limited interactions, with PE/PU showing positive enthalpy of mixing. Electronic study demonstrates PE/PU's higher energy gap of 9.19 eV, correlating with superior performance.

This research contributes to the fundamental understanding of oil absorption processes and informs the design and optimization of environmentally sustainable and efficient oil-absorbing materials for remediation applications.

Highlights

- DFT explores polymeric systems, PE/PU and PE/hexane, for oil absorbent.
- PE/PU excels with −12.87 kcal/mol adsorption energy, surpassing PE/hexane (−7.66 kcal/mol).
- NCI validates van der Waals forces in both systems, crucial for effective adsorption.
- Miscibility studies reveal limited interactions.
- PE/PU's superior 9.19 eV energy gap signifies enhanced absorbent performance.
- PE/PU excels as an oil-absorbent material, underlining its overall superiority.

1 | INTRODUCTION

In recent years, the escalating frequency of oil spill incidents and industrial wastewater discharges has underscored the critical need for effective remediation strategies to mitigate environmental damage.[1–3] Among the various approaches, the utilization of polymeric absorbent materials has gained considerable attention due to their potential to selectively capture and separate oil from water.[4–7] In particular, the integration of low-density polyethylene (LDPE) and polyurethane (PU) materials has shown promising results in oil–water separation, owing to their unique surface properties and robust hydrophobic characteristics.[2,5]

Various studies highlight the inherent hydrophobicity of LDPE, positioning it as a potential material for oil absorption applications.[8,9] Mohamed et al.[8] demonstrate the effectiveness of hydrophobic polymer blends, specifically PS-PE5 and PS-PVC5, in efficiently removing crude oil spills from aqueous media. Thamer et al.[10] developed a nano-adsorbent, the polyethylene (PE)/Fe-MWCNTs nanocomposite, exhibiting superior kerosene adsorption capacity (3560 mg/g) and removal efficiency (71.2%). The study involved functionalizing multiwalled carbon nanotubes (MWCNTs) with nitric acid, depositing Fe_3O_4 nanoparticles, and incorporating PE, showcasing a uniform and homogeneous adsorption process.

The integration of PU, known for its flexibility, durability, and chemical resistance, enhances the absorbent capabilities of LDPE.[11,12] PU has demonstrated widespread use as an adsorbent for oil spillage.[13–16] Larissa et al.[15] developed PU composites with Australian palm residues (PR), with PU-20% PR exhibiting improved

environmental performance, smaller pore sizes, higher oil adsorption capacity (30.39 g/g), and excellent reusability. Similarly, Santos et al.[17] explored lignin concentration as a filler in polyurethane foam (PUF), with PUF-10 showing a 35.5% enhancement in oil sorption capacity compared to PUF-blank. The synergistic combination of PE and PU is envisioned to provide a versatile platform for developing efficient, tailored oil-absorbing materials under specific environmental conditions.

Polymeric sorbents have been effectively utilized for the removal and separation of organic solvents, such as n-hexane, n-hexadecane, and toluene.[18] Hexadecane and its isomers, common components in products like lubricants and fuels, were investigated by Zhaoyun et al.[19] Using a bamboo charcoal–PU composite biofilter, they achieved increased removal efficiency for n-hexane (from 59.4% to 83.1%) and demonstrated potential applications for co-degradation of other volatile organic pollutants in the pharmaceutical industry. Zhixiang and colleagues[20] developed a 3-D porous thermoplastic PU/titania/polydopamine composite foam with remarkable oil/water separation and photocatalytic capabilities. This multifunctional foam displayed high separation efficiency under gravitational force and maintained efficient separation even after multiple cycles, showing promise for addressing environmental threats posed by industrial organic pollutants like n-hexane. Additionally, Jianjia et al.[18] created a robust porous PU hydrogel with ultralow-oil-adhesion properties, capable of highly efficient gravity-driven separation of various oil–water mixtures, including hexadecane oil–water systems, while maintaining durability under
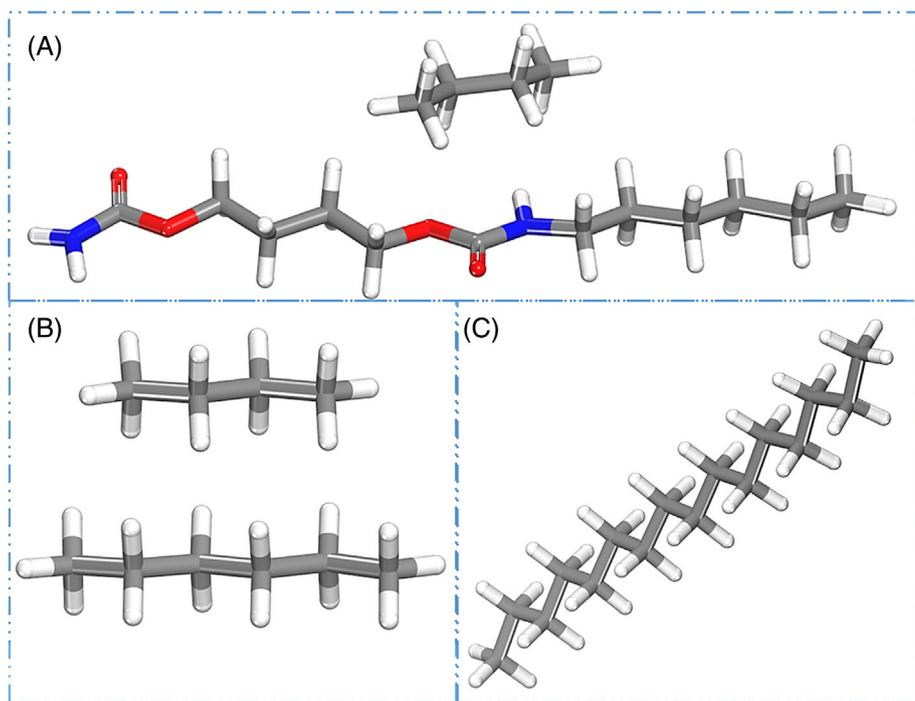
FIGURE 1 3D stick structure of the optimized configuration of the absorbents and the oil. (A) PE/PU absorbent, (B) PE/hexane absorbent, and (C) n-hexadecane. Here red, gray, white, and blue represent oxygen, carbon, hydrogen, and nitrogen, respectively.

harsh conditions, such as exposure to acidic and basic media and mechanical abrasion.

In this context, computational techniques, particularly density functional theory (DFT), have emerged as indispensable tools for unraveling the intricate molecular interactions within absorbent systems.[1,21–23] By employing DFT, one can gain valuable insights into the electronic structure, energetics, and binding characteristics of LDPE-based absorbents with various oil constituents. This computational approach not only complements experimental investigations but also provides a fundamental understanding of the underlying mechanisms governing oil absorption processes.[24–27]

Taking these into account, this study embarks on a comprehensive computational investigation utilizing DFT to elucidate the interaction mechanisms of PE in conjunction with PU and hexane for n-hexadecane removal. By probing the electronic structure and energetics of these systems, we aim to provide valuable insights that will inform the design and optimization of LDPE-based absorbents for effective oil spill remediation. The outcomes of this research hold significant promise for advancing the development of environmentally sustainable and efficient oil-absorbing materials.

2 | COMPUTATIONAL METHOD

Computational investigations were performed using DFT as implemented in the Materials Studio 2020 software package. To reduce the computational demands for DFT calculations, dimers of the polymers (PE and PU), each consisting of two repeating units, were utilized.[28] Hence, the initial structures of the PE/PU and PE/hexane systems were constructed using polymer builder and adsorption locator module (Figure 1), optimizing geometries at the B3LYP level of theory using DMol^3 calculator. The DNP (4.4) basis set was chosen for its balanced accuracy and computational cost. Grimme DFT dispersion correction was employed for the interaction study.

The interaction energies between PE and PU, as well as PE and hexane, were determined by calculating the energy difference between the optimized complex and the sum of the energies of the isolated monomers/constituents. The adsorption energy (E_β) was calculated using Equation (1), which takes into account the energy of the sorbent/oil complex ($E_{sorbent/oil}$), the energy of the sorbent ($E_{sorbent}$), and the energy of the oil (E_{oil}). The negative value of E_β indicates that the adsorption process is exothermic, reflecting the release of energy during the interaction between the absorbents and n-hexadecane.

$$E_b = E_{sorbent/oil} - (E_{sorbent} + E_{oil}) \qquad (1)$$

The charge transfer within the PE/PU and PE/hexane systems was analyzed using the Mulliken population analysis. Electrostatic potentials were mapped to visualize regions of high electron density.

The non-covalent interactions (NCIs), including van der Waals, hydrogen bonding, and π–π stacking, were evaluated using the NCI index. The calculation employs Equation (2) as implemented in Multwfn software.

$$\text{RDGs} = \frac{1}{2(3\pi^2)^{\frac{1}{3}}} \frac{\left|\overline{\Delta\rho(r)}\right|}{\rho(r)^{\frac{4}{3}}}. \qquad (2)$$

Electronic properties, such as highest occupied molecular orbital (HOMO) and lowest unoccupied molecular orbital (LUMO) energies, were computed in Materials Studio to gain insights into the electronic structure and reactivity of the absorbent systems. The energy gap between the ground state and the excited state for each system is calculated using (Equation 3). All geometry optimizations and frequency calculations were considered converged when the maximum force and maximum displacement were below 0.002 Hartree/Å and 0.005 Å, respectively.

$$E_g = E_{HOMO} - E_{LUMO}. \qquad (3)$$

To assess the miscibility of LDPE with PU and hexane, the systems were simulated using blend module in Materials Studio using COMPASSIII forcefield. The total energies and enthalpies of mixing were calculated (Equation 4) to determine the most thermodynamically stable configurations.

$$E_{mix} = \frac{1}{2}z(E_{bs} + E_{sb} - E_{bb} - E_{ss}). \qquad (4)$$

To accurately determine the thermodynamic properties of the studied structures, the DMol3 software employing a gradient-corrected functional (B3LYP) was utilized. The changes in Gibbs free energy (ΔG, Kcal/mol) and enthalpy (ΔH, Kcal/mol) of the sorbate and oil at room temperature were computed using (Equations 5 and 6), respectively. In these equations, $G_{TCorr}^{298.15}$ and $H_{TCorr}^{298.15}$ represent the finite temperature corrections for the Gibbs free energy and enthalpy at 298.15 K for the various components.

$$\Delta G^{298.15K} = \begin{array}{l} 627.51 \left[G_{TCorr}^{298.15}(\text{complex}) \right. \\ \left. - \left[G_{TCorr}^{298.15}(\text{adsorbent}) + G_{TCorr}^{298.15}(\text{oil}) \right] \right]. \end{array} \qquad (5)$$

$$\Delta H^{298.15K} = \begin{array}{l} 627.51 \left[H_{TCorr}^{298.15}(\text{complex}) \right. \\ \left. - \left[H_{TCorr}^{298.15}(\text{adsorbent}) + H_{TCorr}^{298.15}(\text{oil}) \right] \right]. \end{array} \qquad (6)$$

3 | RESULTS AND DISCUSSION

3.1 | Interaction study

3.1.1 | Adsorption energies

In the investigation of adsorption energies within the PE/PU and PE/hexane systems, we aimed to understand the strength of the interaction between the absorbents and n-hexadecane, shedding light on their potential as absorbent materials for oil spill remediation.

The classical adsorption energies, representing the energy change during the adsorption process, were calculated for both systems. The LDPE/PU system exhibited a notably higher adsorption energy of −12.87 kcal/mol compared to the LDPE/hexane system at −7.66 kcal/mol. This substantial difference indicates a stronger binding affinity in the LDPE/PU-n-hexadecane complex, suggesting its superiority in terms of oil adsorption.

The optimized 3D stick structures (Figure 2) visually illustrate the spatial arrangement of the absorbents and oil complexes. In the LDPE/PU-n-hexadecane complex, the optimized configuration displayed a shorter distance between LDPE, PU, and n-hexadecane (2.08 and 1.95 Å), implying a more compact and efficient arrangement for adsorption. Conversely, the LDPE/hexane-n-hexadecane complex exhibited slightly longer distances (2.12, 2.08, and 1.95 Å), indicative of weaker interactions and less effective adsorption.

3.1.2 | Intermolecular interactions

Charge transfer and electrostatic interactions
The calculations for atomic charge transfer provide insights into how charges are distributed within the PE/PU and PE/n-hexane systems when interacting with n-hexadecane oil. As illustrated in Figure 3, the observed charge transfer is minimal and appears to occur randomly. This limited and erratic charge transfer is consistent with the expected behavior in van der Waals interactions. Van der Waals forces, being typically nonpolar, are characterized by temporary fluctuations in electron density.

Therefore, the results suggest that the primary driving force for the adsorption of n-hexadecane is likely attributed to non-covalent van der Waals forces. These forces involve induced dipoles and London dispersion forces, emphasizing the importance of non-polar interactions in the adsorption process.

To gain insight into the electrostatic interactions within the PE/PU and PE/hexane systems, we employed molecular electrostatic potential (MEP) maps. These maps, reflecting the distribution of electronic density in molecules, are pivotal in discerning sites of positive and negative electrostatic potentials, crucial for understanding nucleophilic and electrophilic reactions.[29]

Figure 3 presents the MEP maps for the PE/PU-n-hexadecane and PE/hexane-n-hexadecane complexes. In these maps, red and orange regions indicate negative electrostatic potentials, associated with high electron
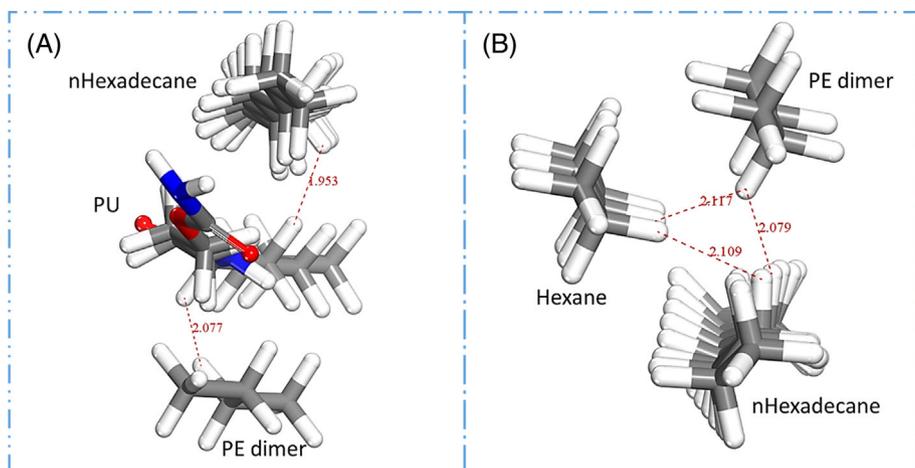
FIGURE 2 3D stick structure of the optimized configuration of the absorbents and the oil complexes. (A) PE/PU-n-hexadecane complex and (B) PE/hexane-n-hexadecane complex.
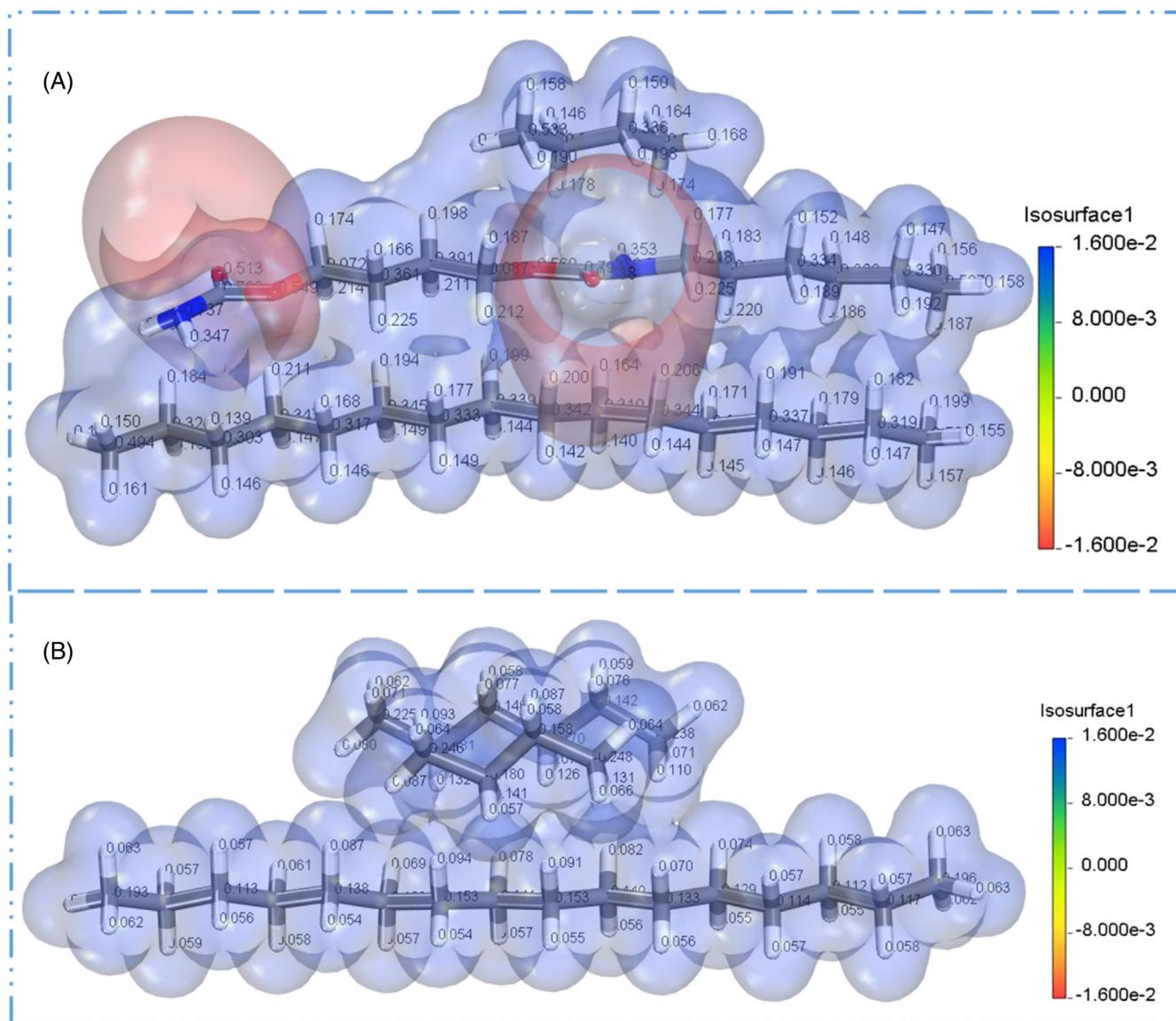

FIGURE 3 Molecular electrostatic potential (MEP) surfaces of the optimized structures of the (A) PE/PU-n-hexadecane complex and (B) PE/hexane-n-hexadecane complex.

density, suggesting electrophilic reactivity. Conversely, blue and green regions represent positive potentials, indicative of low electron density and nucleophilic reactivity. Neutral zones are depicted in light yellow-green.[30–32]

In the LDPE/PU-n-hexadecane complex, dominant negative potentials are observed over the electronegative oxygen and nitrogen atoms. This correlates with the higher adsorption energy observed in the PE/PU system, as these negative regions contribute to the attractive forces between PE/PU and n-hexadecane. In contrast, the PE/hexane-n-hexadecane complex shows dominant positive potentials over the carbon and hydrogen atoms. This suggests weaker electrostatic interactions, aligning with the lower adsorption energy in the LDPE/hexane system.

The analysis of electrostatic potentials provides a molecular-level understanding of the nature of interactions. The dominant negative potentials in the PE/PU-n-hexadecane complex substantiate the enhanced affinity of PE/PU for n-hexadecane compared to LDPE/hexane. This information complements the adsorption energy results, offering a nuanced perspective on the electrostatic contributions to the overall interaction mechanisms.

Electrostatic interactions play a pivotal role in dictating the adsorption behavior, and these findings contribute to the broader comprehension of the studied systems. The subsequent section will delve into NCIs, providing a more comprehensive view of the forces governing the adsorption of oil onto the absorbent materials.

Non-covalent interaction

To further elucidate the NCIs governing the PE/PU and PE/hexane systems, we conducted an in-depth analysis employing the reduced density gradient (RDG; Equation 2) and Sign(λ_2)*ρ function. These tools allowed us to explore regions of weak interactions, providing valuable insights into the nature and strength of non-covalent forces.[33] The RDG isosurfaces, color-coded to represent the intensity and nature of interactions, are depicted in Figure 4. Blue isosurfaces signify strong NCIs, green represents Van der Waals interactions, and red indicates strong repulsive forces, such as steric hindrance.

The scatter plots and RDG isosurface maps for PE/PU-n-hexadecane and PE/hexane-n-hexadecane complexes (Figure 4) underscore the presence of weaker van der Waals interactions, reinforcing their significant role in the adsorption process. The green isosurface regions in the PE/PU-n-hexadecane complex, corresponding to Van der Waals forces, are indicative of attractive interactions between PE and PU. In contrast, the PE/hexane-n-hexadecane complex exhibits weaker van der Waals interactions.

The NCI analysis corroborates the earlier findings from the electrostatic interactions section, providing a

more detailed view of the forces contributing to adsorption. The green regions in the PE/PU-n-hexadecane complex align with the negative electrostatic potentials over the electronegative oxygen and nitrogen atoms, forming a cohesive framework of attractive forces. In the PE/hexane-n-hexadecane complex, weaker van der Waals interactions correspond to the positive electrostatic potentials over carbon and hydrogen atoms, consistent with the less favorable adsorption energies observed.

The comprehensive understanding of NCIs enhances our grasp of the intricate mechanisms underlying the adsorption process. These weak forces, particularly Van der Waals interactions, play a pivotal role in stabilizing the PE/PU-n-hexadecane complex, contributing to its superior adsorption affinity.

3.2 | Miscibility study

The miscibility study aimed to unravel the blending behavior of PE/PU and PE/hexane systems with n-hexadecane. This investigation is crucial for understanding the potential of these systems as effective oil-absorbent materials.

Our analysis revealed that both the PE/PU and PE/hexane absorbents, when in contact with n-hexadecane, exhibited limited interactions. This conclusion is drawn from the positive enthalpy of mixing, signifying an endothermic process. The positive enthalpy indicates that the absorbents do not possess a strong tendency to form a homogeneous blend with n-hexadecane. In oil spill remediation scenarios, the formation of a homogeneous blend is essential for an absorbent material to effectively encapsulate and remediate spilled oil.

Furthermore, we delved into estimating the binding energy distribution in our study. The energy of contact between the oil and the polymer adsorbents was measured by the binding energy, allowing the creation of phase diagrams, mixing energy evaluations, and the chi parameter calculation when combined with the coordination numbers (Z).

Figure 5 illustrates the binding configuration of both the PE/PU absorbent with n-hexadecane and the PE/hexane absorbent with n-hexadecane. The adsorbents played the role of the base in the blend simulation, while the oil served as the screen. Four distinct pairs were identified: base–base pair (E_{bb}), screen–screen pair (E_{ss}), base–screen pair (E_{bs}), and screen–base pair (E_{sb}). Each pair had a corresponding binding energy value, and the energy of the mixture was expressed in terms of these binding energies and the coordination numbers (Z) for each pair, as per Equation (4).
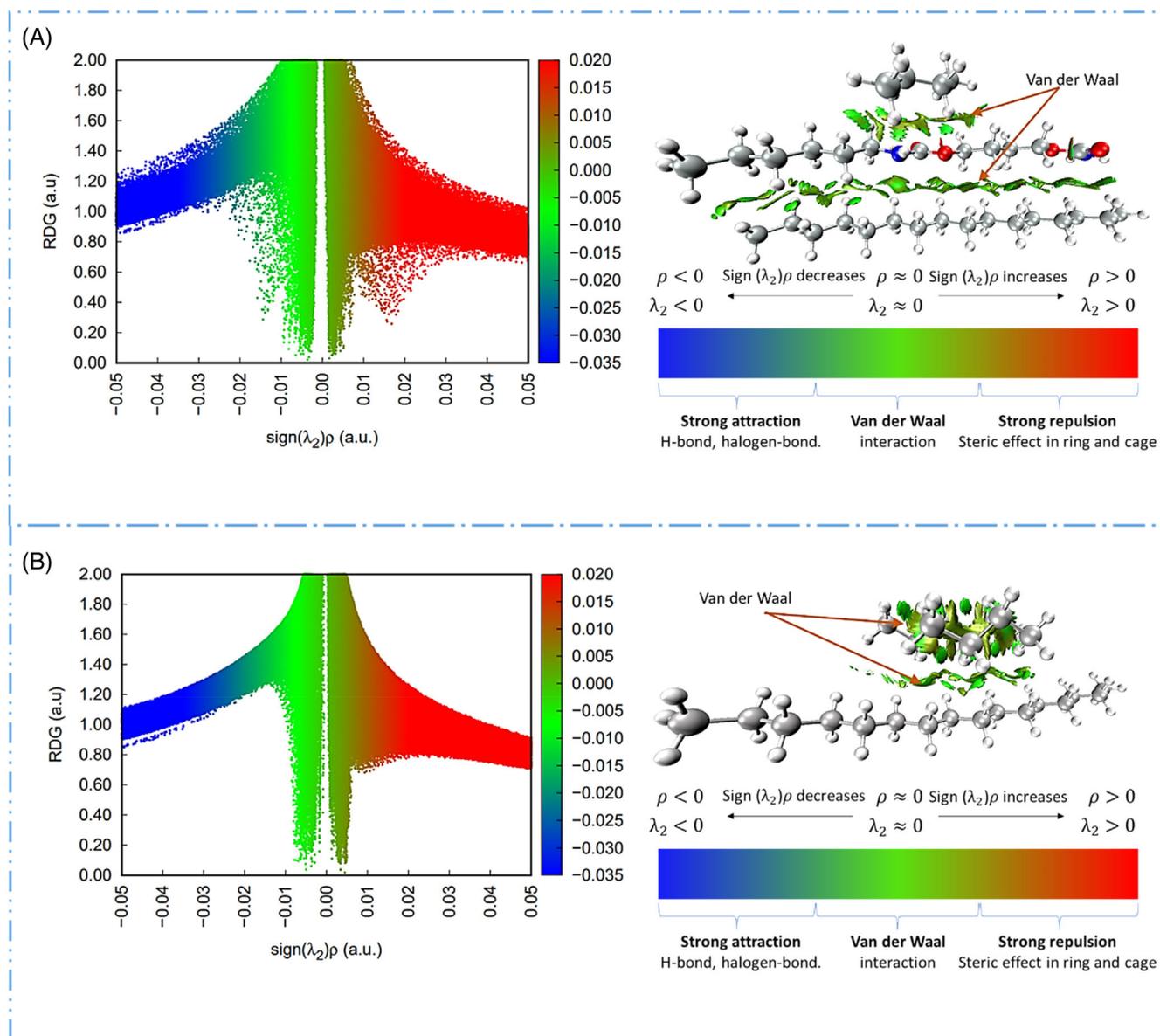
FIGURE 4 Scatter plot (left) and reduced density gradient (RDG) isosurface map (right) for the visualization of the noncovalent interactions of (A) LDPE/PU-n-hexadecane complex and (B) LDPE/hexane-n-hexadecane complex.

To gain insights into the temperature dependence of complex immiscibility, we examined the chi parameter versus temperature plot for PE/PU absorbent with n-hexadecane and PE/hexane absorbent with n-hexadecane (Figure A7). In a scenario where the interaction parameter is positive, indicating that a mixed state is not preferred by the adsorbent–oil system, the chi parameter drops as temperature rises. This observation suggests that the complex is immiscible at elevated temperatures.

Table 1 summarizes the blending parameters for the PE/PU and PE/hexane systems with n-hexadecane. The chi values at 298 K for PE/PU-n-hexadecane and PE/hexane-n-hexadecane are 11.35 and 7.63, respectively. These positive chi values further affirm the immiscibility of the absorbent–oil systems (Figure 6).

3.3 | Electronic and thermodynamic study

The electronic study focused on the energy of frontier molecular orbitals, specifically the LUMO and the HOMO, to calculate chemical descriptors and investigate the electronic properties of the PE/PU and PE/hexane systems with n-hexadecane. Figure 7A,B depict the HOMO and LUMO orbitals of the optimized PE/PU-n-hexadecane complex and PE/hexane-n-hexadecane complex structures, respectively.

In the PE/PU-n-hexadecane complex, the HOMO orbital is predominantly localized on (-C-O-), (-C-N-), and (-C=O) of the urethane structure and (-N-H) of the amino group. Meanwhile, the LUMO orbital is

FIGURE 5 Binding configuration of (A) PE/PU absorbent with n-hexadecane and (B) PE/hexane absorbent with n-hexadecane.
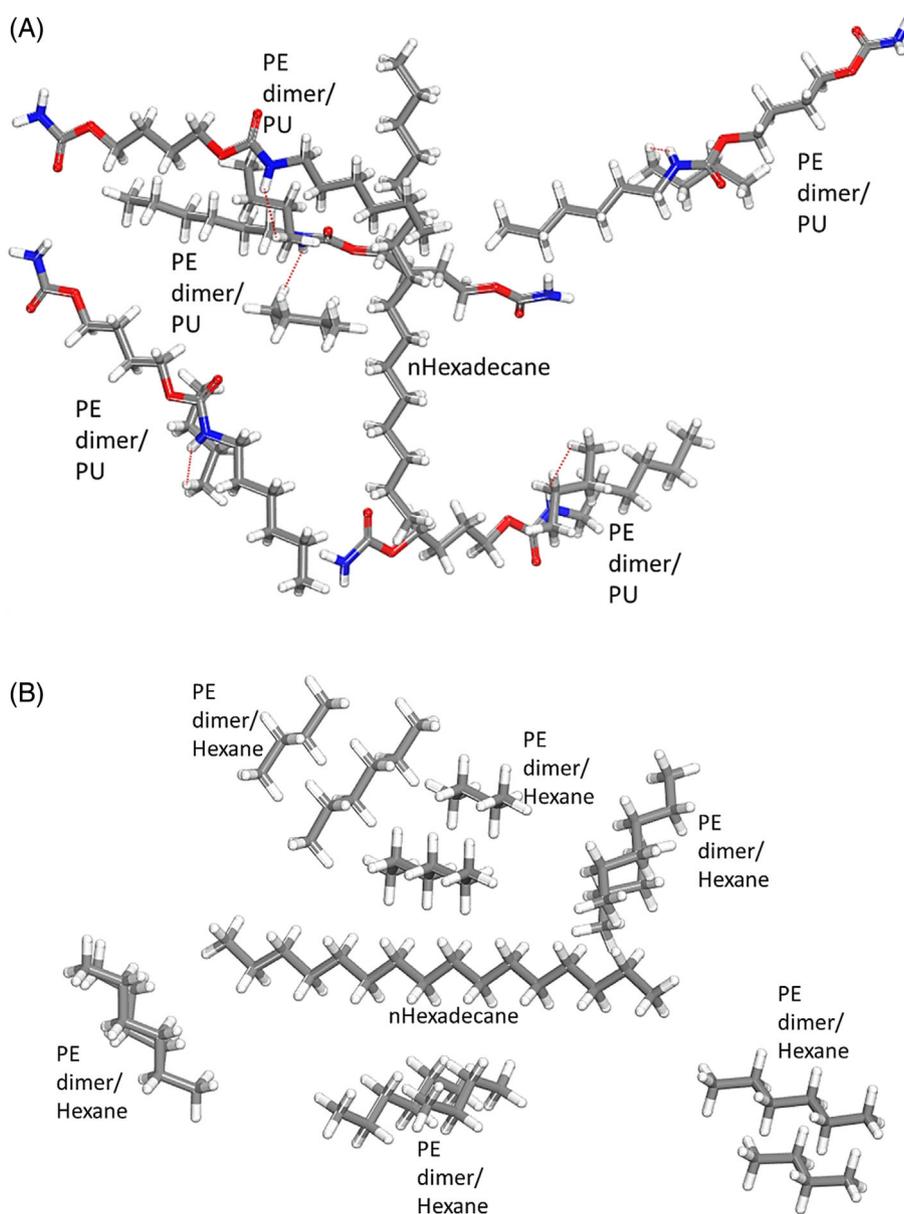

TABLE 1 Blending parameters for the adsorbent–oil system.

Systems	Chi (298 K)	E_{mix} (298 K)	E_{bb} avg (298 K)	E_{bs} avg (298 K)	E_{ss} avg (298 K)	Z_{bb}	Z_{bs}	Z_{sb}	Z_{ss}
PE/PU-n-H	11.35	6.72	−6.27	−3.89	−3.94	5.54	5.62	5.38	5.48
PE/H-n-H	7.63	4.52	−2.01	−2.23	−4.10	5.55	4.45	6.56	5.49

found on the edge (-C-O-), (-C-N-), and (-C=O) of the urethane structure. This suggests that the interaction sites involve the urethane groups, indicating a specific molecular interaction between LDPE/PU and n-hexadecane.

Conversely, in the PE/hexane-n-hexadecane complex, the HOMO orbitals are predominantly located on the (-C-C-) of n-hexadecane. The LUMO, on the other hand, is predominantly located on some of the (-C-C-) of n-hexadecane and PE/hexane. This implies that the interaction in the PE/Hexane system primarily occurs at the hydrocarbon backbone.

The energy gap (Eg) for each complex was calculated using Equation (4). The energy gap provides insights into the stability and reactivity of a system. For the PE/PU-
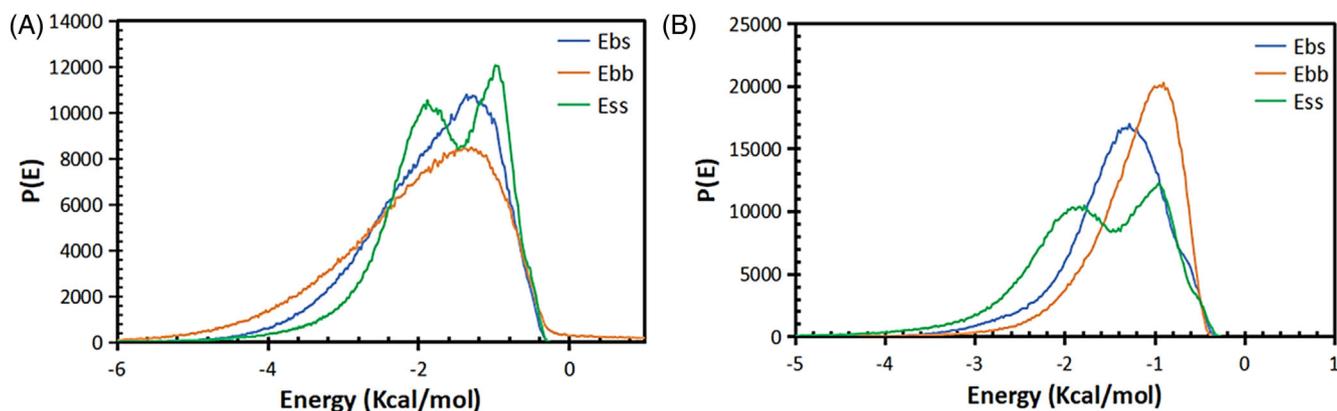
FIGURE 6 The mixture binding energy distribution for (A) PE/PU absorbent with n-hexadecane and (B) PE/hexane absorbent with n-hexadecane.

n-hexadecane complex, the energy gap is 9.19 eV, while for PE/hexane-n-hexadecane, it is 7.91 eV. The PE-n-hexadecane complex has an energy gap of 9.48 eV.

The HOMO–LUMO analysis indicates that PE/hexane exhibits a narrower energy gap compared to PE/PU. A narrower energy gap signifies higher reactivity and lower stability, suggesting that the PE/hexane system is more prone to chemical reactions compared to PE/PU.

The electronic study provides valuable insights into the specific molecular interactions between the absorbents and n-hexadecane. The localization of HOMO and LUMO orbitals on functional groups and hydrocarbon backbones indicates the nature of the interactions. The higher energy gap in PE/PU suggests greater stability, which aligns with the superior performance observed in the adsorption and miscibility studies. These electronic properties contribute to the overall understanding of the PE/PU and PE/hexane systems as absorbents for oil spill remediation.

$$E_g = E_{HOMO} - E_{LUMO}. \qquad (7)$$

The Gibbs free energy change (ΔG) is a crucial parameter in understanding the spontaneity of oil absorption processes.[34] Our investigation into the PE/hexane-n-hexadecane and PE/PU-n-hexadecane complexes at 298.15 K yielded ΔG values of -34.79 kcal/mol and -42.54 kcal/mol, respectively. Table 2 presents the values for the total energy (E_{tot}), enthalpy change (ΔH), and Gibbs free energy change (ΔG) for the polymer absorbent systems. Negative ΔG values for both complexes indicate the spontaneous nature of the adsorption process. Notably, the PE/PU complex exhibited a lower ΔG, suggesting a more favorable and spontaneous oil absorption compared to the PE/hexane system. This aligns with the reported spontaneous behavior observed in the removal of methylene blue using alginate, where the ΔG is measured at -97.58 kcal/mol.[35]

The enthalpy change (ΔH) provides insights into the strength of intermolecular interactions during oil absorption. Our findings revealed ΔH values of -55.75 kcal/mol for PE/hexane-n-hexadecane and -66.11 kcal/mol for PE/PU-n-hexadecane complexes at 298.15 K. Both complexes exhibited negative ΔH values, indicating exothermic adsorption. The more exothermic ΔH observed for PE/PU signifies stronger interactions during the oil absorption process compared to PE/hexane.

The combined analysis of ΔG and ΔH underscores the superior performance of the PE/PU system as an oil-absorbent material. The lower ΔG for PE/PU indicates a higher likelihood of spontaneous oil absorption, while the more exothermic ΔH suggests enhanced molecular interactions. These thermodynamic characteristics align with our earlier findings of PE/PU exhibiting significantly higher adsorption energies and affirm its efficacy in oil spill remediation.

In practical terms, these thermodynamic insights suggest that PE/PU not only possesses a higher affinity for n-hexadecane but also exhibits a more favorable and spontaneous oil absorption process. These findings contribute valuable information for the design and optimization of advanced absorbent materials, emphasizing the importance of molecular-level understanding in the development of efficient and environmentally sustainable solutions for oil spill remediation.

4 | CONCLUSION

The computational exploration of PE/PU and PE/hexane systems for oil spill remediation, utilizing DFT, offers insights into molecular interactions, miscibility, and electronic properties. PE/PU exhibits superior adsorption energy (-12.87 kcal/mol) compared to PE/hexane (-7.66 kcal/mol), aligning with enhanced oil absorbency

FIGURE 7 Highest occupied molecular orbital (HOMO) and lowest unoccupied molecular orbital (LUMO) structures of (A) PE/PU-n-hexadecane complex, and (B) PE/hexane-n-hexadecane complex.
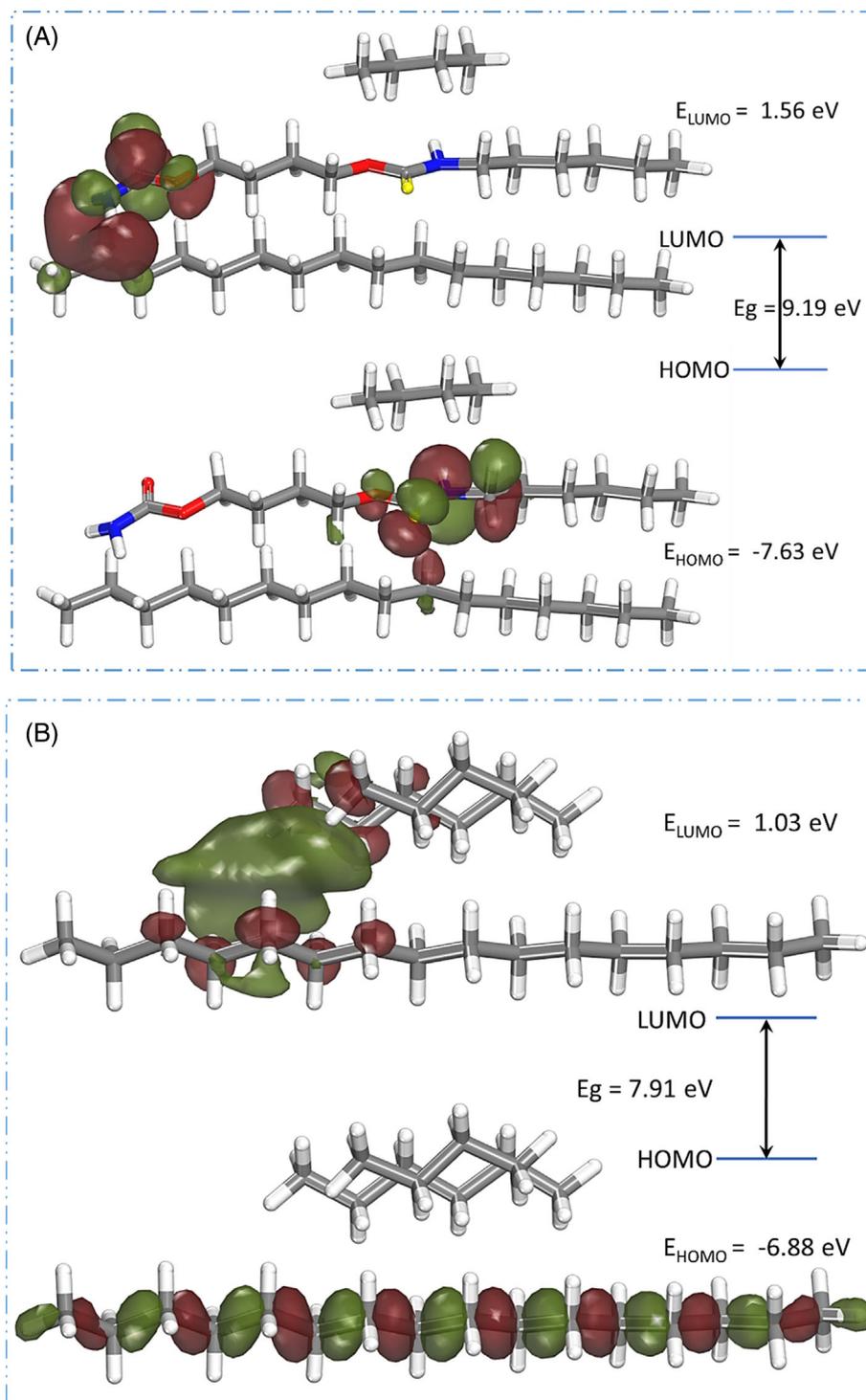

TABLE 2 Thermodynamic parameters for the polymeric absorbent systems.

Structure configuration	E_{tot} (Ha)	$H_{TCorr}^{298.15}$ (Ha)	$\Delta H^{298.15K}$ (Kcal/mol)	$G_{TCorr}^{298.15}$ (Ha)	$\Delta G^{298.15K}$ (Kcal/mol)
PE/H	−419.76	−419.42	-	−419.48	-
PE/PU	−1101.60	−1101.07	-	−1101.16	-
nH	−668.97	−668.48	-	−668.55	-
PE/H-nH	−1088.82	−1087.99	−55.75	−1088.09	−34.79
PE/PU-nH	−1770.68	−1769.66	−66.11	−1769.78	−42.54

observed experimentally. Electrostatic analysis shows PE/PU-n-hexadecane with dominant negative potential, supporting its higher adsorption energy, while PE/hexane-n-hexadecane displays positive potential, indicating weaker adsorption. The enthalpy results indicate exothermic adsorption for both PE/hexane-n-hexadecane and PE/PU-n-hexadecane complexes at 298.15 K. The more exothermic ΔH in PE/PU suggests stronger interactions during oil absorption compared to PE/hexane. Additionally, Gibbs free energy change (ΔG) values confirm a more favorable process for PE/PU, with a lower ΔG (-42.54 kcal/mol) compared to PE/hexane (-34.79 kcal/mol). NCI analysis confirms van der Waals forces in both systems, crucial for the adsorption process. Miscibility studies reveal limited interactions, vital for designing effective oil-absorbent materials. Electronic analysis indicates PE/PU's higher energy gap, suggesting greater stability and correlating with its superior performance. The study provides a scientific foundation for designing advanced absorbents, with PE/PU identified as promising for addressing oil spill environmental challenges. Future research could explore further improvements in PE/PU for enhanced adsorption efficiency and miscibility.

ACKNOWLEDGMENTS

CONFLICT OF INTEREST STATEMENT
The authors declare no conflict of interest.

DATA AVAILABILITY STATEMENT
Data is available on request.

ORCID
Anthony Chidi Ezika https://orcid.org/0000-0001-9426-678X

REFERENCES

1. Tella AC, Owalude SO, Ameen OA, et al. Synthesis, crystal structures and DFT studies of Co(ii) and Zn(ii) coordination polymers of terephthalate and 4,4′-trimethylenedipyridyl ligands for removal of dibenzothiophene from a model fuel oil. *CrystEngComm*. 2023;25(28):3998-4010. doi:10.1039/D3CE00236E

2. Wang Z, Hu L, Zhao M, et al. Bamboo charcoal fused with polyurethane foam for efficiently removing organic solvents from wastewater: experimental and simulation. *Biochar*. 2022;4(1):28. doi:10.1007/s42773-022-00153-2

3. Geng T, Chen H, Xu J, Ren M, Liu J, Cao F. Removal of nickels from crude oil to water by two micro-sized core-shell particles bearing poly(N-vinyl pyrrolidone). *Fuel*. 2019;245:181-187. doi:10.1016/j.fuel.2019.02.053

4. Geng T, Xu J, Ren M, Li X, Cao F. Selectivity and capacity of the core-shell demetalizers for removal of nickel and calcium

5. ions from heavy oil through conventional electric desalination process. *Fuel*. 2021;289:119935. doi:10.1016/j.fuel.2020.119935

5. Yang J, Loh XJ, Tan BH, Li Z. pH-responsive poly(dimethylsiloxane) copolymer decorated magnetic nanoparticles for remotely controlled oil-in-water Nanoemulsion separation. *Macromol Rapid Commun*. 2019;40(5):1800013. doi:10.1002/marc.201800013 (Accessed November 9, 2023).

6. Mathidala S, Ogunlaja AS. Selective removal of pyridine in fuel by imprinted polymer (poly 4-vinyl aniline-co-DVB) as adsorbent. *Pet Sci Technol*. 2019;37(14):1691-1703. doi:10.1080/10916466.2019.1602641

7. Chen J, Chen S. Removal of polycyclic aromatic hydrocarbons by low density polyethylene from liquid model and roasted meat. *Food Chem*. 2005;90(3):461-469. doi:10.1016/j.foodchem.2004.05.010

8. Alnaqbi MA, Al Blooshi AG, Greish YE. Polyethylene and polyvinyl chloride-blended polystyrene nanofibrous sorbents and their application in the removal of various oil spills. *Adv Polym Technol*. 2020;2020:4097520. doi:10.1155/2020/4097520 12.

9. Abdullah TA, Juzsakova T, Mansoor H, et al. Polyethylene over magnetite-multiwalled carbon nanotubes for kerosene removal from water. *Chemosphere*. 2022;287:132310. doi:10.1016/j.chemosphere.2021.132310

10. Abdullah TA, Juzsakova T, Rasheed RT, et al. V_2O_5, CeO_2 and their MWCNTs nanocomposites modified for the removal of kerosene from water. *Nanomaterials*. 2022;12:189.

11. Li Z, Chen K, Chen Z, et al. Removal of malachite green dye from aqueous solution by adsorbents derived from polyurethane plastic waste. *J Environ Chem Eng*. 2021;9(1):104704. doi:10.1016/j.jece.2020.104704

12. Zhang S, Chen S, Li H, Lai X, Zeng X. Superhydrophobic, flame-retardant and magnetic polyurethane sponge for oil-water separation. *J Environ Chem Eng*. 2022;10(3):107580. doi:10.1016/j.jece.2022.107580

13. Zhang T, Kong L, Zhang M, Qiu F, Rong J, Pan J. Synthesis and characterization of porous fibers/polyurethane foam composites for selective removal of oils and organic solvents from water. *RSC Adv*. 2016;6(89):86510-86519. doi:10.1039/C6RA10916K

14. Costa RMD d, Hungerbühler G, Saraiva T, et al. Green polyurethane synthesis by emulsion technique: a magnetic composite for oil spill removal. *Polimeros*. 2017;27:273-279.

15. Martins LS, Zanini NC, Maia LS, et al. Crude oil and S500 diesel removal from seawater by polyurethane composites reinforced with palm fiber residues. *Chemosphere*. 2021;267:129288. doi:10.1016/j.chemosphere.2020.129288

16. de Nino A, Olivito F, Algieri V, et al. Efficient and fast removal of oils from water surfaces via highly oleophilic polyurethane composites. *Toxics*. 2021;9:186.

17. Santos OSH, Coelho da Silva M, Silva VR, Mussel WN, Yoshida MI. Polyurethane foam impregnated with lignin as a filler for the removal of crude oil from contaminated water. *J Hazard Mater*. 2017;324:406-413. doi:10.1016/j.jhazmat.2016.11.004

18. Huang J, Zhang Z, Weng J, et al. Molecular understanding and design of porous polyurethane hydrogels with ultralow-oil-adhesion for oil–water separation. *ACS Appl Mater Interfaces*. 2020;12(50):56530-56540. doi:10.1021/acsami.0c18825

19. Wang Z, Hu L, He J, et al. Mechanisms of *N, N*-dimethylacetamide-facilitated n-hexane removal in a rotating drum biofilter

packed with bamboo charcoal-polyurethane composite. *Bioresour Technol*. 2023;372:128600. doi:10.1016/j.biortech.2023.128600

20. Cui Z, Marcelle SSA, Zhao M, et al. Thermoplastic polyurethane/titania/polydopamine(TPU/TiO2/PDA) 3-D porous composite foam with outstanding oil/water separation performance and photocatalytic dye degradation. *Adv Compos Hybrid Mater*. 2022;5(4):2801-2816. doi:10.1007/s42114-022-00503-5

21. Adekoya OC, Adekoya GJ, Sadiku ER, Hamam Y, Ray SS. Application of DFT calculations in designing polymer-based drug delivery systems: an overview. *Pharmaceutics*. 2022;14(9):1972.

22. Mahdavian L. DFT study on the removal of polyacrylamide by titanium dioxide nanoparticles/polyacrylonitrile (rTiO2@PAC) composite in aqueous solutions. *J Mol Model*. 2022;28(12):396. doi:10.1007/s00894-022-05390-7

23. Li L, Yu X, Yang X, et al. Porous BN with vacancy defects for selective removal of CO from H2 feed gas in hydrogen fuel cells: a DFT study. *J Mater Chem A*. 2016;4(40):15631-15637. doi:10.1039/C6TA03208G

24. Adekoya OC, Adekoya GJ, Sadiku RE, Hamam Y, Ray SS. Density functional theory interaction study of a polyethylene glycol-based nanocomposite with cephalexin drug for the elimination of wound infection. *ACS Omega*. 2022;7(38):33808-33820.

25. Adekoya GJ, Folorunso O, Adekoya OC, Hamam Y, Sadiku ER, Ray SS. *Adsorption of EDOT on Graphene: DFT and MC Studies*. Vol 2607. AIP Publishing; 2023.

26. Adekoya GJ, Sadiku ER, Hamam Y, Mwakikunga BW, Ray SS. *DFT and MC Investigation of EDOT on Honeycomb Borophene as Potential Energy Storage Material*. Vol 2607. AIP Publishing; 2023.

27. Ezika AC, Sadiku ER, Ray SS, Hamam Y, Adekoya GJ. MXene/PPy nanocomposite as an electrode material for high-capacity Na-ion batteries investigated from first principle calculation. *S Afr J Chem Eng*. 2023;44(1):297-301.

28. Ezika AC, Sadiku ER, Adekoya GJ, Ray SS, Hamam Y. Quantum mechanical study of the dielectric response of V2C-ZnO/PPy ternary nanocomposite for energy storage application. *J Inorg Organomet Polym Mater*. 2023;33:1-7.

29. Ekici Ö, Demircioğlu Z, Ersanlı CC, Çukurovalı A. Experimental and theoretical approach: chemical activity, charge transfer of DNA/ECT, thermodinamic, spectroscopic, structural and electronic properties of N-(4-(3-methyl-3-phenylcyclobutyl)thiazol-2-yl)acetamide molecule. *J Mol Struct*. 2020;1204:127513. doi:10.1016/j.molstruc.2019.127513

30. Hesabi M, Behjatmanesh-Ardakani R. Investigation of carboxylation of carbon nanotube in the adsorption of anti-cancer drug: a theoretical approach. *Appl Surf Sci*. 2018;427:112-125. doi:10.1016/j.apsusc.2017.08.044

31. Sheikhi M, Shahab S, Khaleghian M, Kumar R. Interaction between new anti-cancer drug Syndros and CNT(6,6-6) nanotube for medical applications: geometry optimization, molecular structure, spectroscopic (NMR, UV/Vis, excited state), FMO, MEP and HOMO-LUMO investigation. *Appl Surf Sci*. 2018;434:504-513. doi:10.1016/j.apsusc.2017.10.154

32. Bagheri Novir S, Aram MR. Quantum mechanical studies of the adsorption of Remdesivir, as an effective drug for treatment of COVID-19, on the surface of pristine, COOH-functionalized and S-, Si- and Al- doped carbon nanotubes. *Phys E*. 2021;129:114668. doi:10.1016/j.physe.2021.114668

33. Johnson ER, Keinan S, Mori-Sánchez P, Contreras-García J, Cohen AJ, Yang W. Revealing noncovalent interactions. *J Am Chem Soc*. 2010;132(18):6498-6506. doi:10.1021/ja100936w

34. Delley B. From molecules to solids with the DMol3 approach. *J Chem Phys*. 2000;113(18):7756-7764. doi:10.1063/1.1316015 (Accessed November 15, 2021).

35. Allangawi A, Aziz Aljar MA, Ayub K, El-Fattah AA, Mahmood T. Removal of methylene blue by using sodium alginate-based hydrogel; validation of experimental findings via DFT calculations. *J Mol Graph Model*. 2023;122:108468. doi:10.1016/j.jmgm.2023.108468

SUPPORTING INFORMATION

Additional supporting information can be found online in the Supporting Information section at the end of this article.